Proc. Natl. Acad. Sci. USA
Vol. 89, pp. 554–558, January 1992
Medical Sciences

Primary structure and functional expression of the human cardiac tetrodotoxin-insensitive voltage-dependent sodium channel

(complementary DNA/heart muscle/electrophysiology/antiarrhythmic)

MARY E. GELLENS*, ALFRED L. GEORGE, JR.*†, LIQIONG CHEN†, MOHAMED CHAHINE‡, RICHARD HORN‡, ROBERT L. BARCHI†§¶, AND ROLAND G. KALLEN†§‖

Departments of *Medicine, †Biochemistry and Biophysics, ¶Neurology, and the §David Mahoney Institute of Neurological Sciences, University of Pennsylvania, Philadelphia, PA 19104; and ‡Department of Neurosciences, Roche Institute of Molecular Biology, Nutley, NJ 07110

Communicated by Eliot Stellar, September 23, 1991

ABSTRACT **The principal voltage-sensitive sodium channel from human heart has been cloned, sequenced, and functionally expressed. The cDNA, designated hH1, encodes a 2016-amino acid protein that is homologous to other members of the sodium channel multigene family and bears >90% identity to the tetrodotoxin-insensitive sodium channel characteristic of rat heart and of immature and denervated rat skeletal muscle. Northern blot analysis demonstrates an ≈9.0-kilobase transcript expressed in human atrial and ventricular cardiac muscle but not in adult skeletal muscle, brain, myometrium, liver, or spleen. When expressed in *Xenopus* oocytes, hH1 exhibits rapid activation and inactivation kinetics similar to native cardiac sodium channels. The single channel conductance of hH1 to sodium ions is about twice that of the homologous rat channel and hH1 is more resistant to block by tetrodotoxin (IC_{50} = 5.7 μM). hH1 is also resistant to μ-conotoxin but sensitive to block by therapeutic concentrations of lidocaine in a use-dependent manner.**

Voltage-dependent sodium channels (NaChs) form a multigene family, with six isoforms currently identified in the rat (1). Although structurally very similar, these isoforms can be distinguished by their kinetics (2), single-channel conductance (3), toxin sensitivity (4, 5), and reactivity with specific immunoreagents (6). For example, a NaCh isoform expressed in rat cardiac and in immature or denervated adult skeletal muscle differs dramatically from the NaCh in innervated skeletal muscle in its relative insensitivity to block by tetrodotoxin (TTX), saxitoxin, and μ-conotoxin (4, 5, 7).

Tetrodotoxin-insensitive (TTX-I) voltage-dependent NaChs are critical for the initial rapid upstroke of the cardiac action potential and are responsible for most of the Na^+ current that occurs in mammalian heart (8, 9). In addition, this TTX-I NaCh isoform is the principal target of class I (cardiac) antiarrhythmic agents (10). Although NaCh blocking agents of this type are widely used in the acute therapy of ventricular tachyarrhythmias, their precise molecular mechanism of action remains unclear, in part due to the difficulty of studying human cardiac NaChs in isolation.

An *in vitro* expression system for studying isolated human cardiac NaChs would have great utility. However, previous attempts to functionally express cardiac TTX-I NaChs in oocytes using RNA from mammalian heart have met with variable success (11–13). While functional expression of the rat muscle TTX-I isoform (rSkM2) from its cloned cDNA has been accomplished (14), the applicability of these findings to the homologous human cardiac NaCh is unknown. We report here the cloning, sequencing, and functional expression of the TTX-I NaCh from human heart, designated hH1.**

The publication costs of this article were defrayed in part by page charge payment. This article must therefore be hereby marked "*advertisement*" in accordance with 18 U.S.C. §1734 solely to indicate this fact.

MATERIALS AND METHODS

Screening of a Human Cardiac cDNA Library. A size-selected [>1 kilobase (kb)] oligo-(dT) and random-primed adult human cardiac cDNA library constructed in λZAPII (Stratagene) was screened with cDNA probes derived from rSkM2 [nucleotides (nt) 1–4385 and 5424–7076; ref. 15]. Hybridizations were performed at 42°C for 18 h in 50% (vol/vol) formamide/5× SSPE/5× Denhardt's solution/0.1% SDS/salmon sperm DNA (0.15 mg/ml)/random-primed ^{32}P-labeled probe (1.5×10^6 dpm/ml)] and filters were washed with 6× standard saline citrate (SSC)/0.1% SDS at 65°C. (1× SSPE = 0.18 M NaCl/10 mM sodium phosphate, pH 7.4/1 mM EDTA.) Plaque-purified clones were rescued as pBluescript phagemids and sequenced as described (15).

Northern Blot Analysis. Human tissues were obtained as frozen surgical pathology specimens or procured from cadaveric transplant organ donors by the National Disease Research Interchange (Philadelphia, PA). Total cellular RNA was isolated by the method of Chirgwin *et al.* (16). Samples (10 μg) were size-fractionated, electroblotted, and prehybridized as described (15). A subtype-specific hH1 antisense complementary RNA probe derived from clone C92, representing 0.9 kb of the 3′-untranslated (UT) region (nt 7494–8491) was transcribed *in vitro* from *Bam*HI-linearized template DNA and used in Northern blot hybridizations at 5×10^6 dpm/ml. After hybridization (55°C, 18 h), blots were washed at a final stringency of 0.1× SSC/0.1% SDS, 75°C.

Functional Expression in *Xenopus* Oocytes. A full-length hH1 construct was made in pBluescript by sequential ligation of S14 *Eco*RI–*Sac* II (nt +1 to +252), C75 *Sac* II–*Kpn* I (nt +253 to +4377), and C92 *Kpn* I–*Eco*RI (nt +4378 to +8491) fragments and the full-length hH1 insert moved into a modified pSP64T vector (14). nt −151 to −8 of the 5′-UT region were deleted from the construct using exonuclease III and mung bean nuclease (14). A 901-base-pair (bp) *Kpn* I–*Eag* I fragment from clone C21 (nt 4378–5279) was exchanged for the corresponding fragment in pSP64T-hH1 to eliminate a cloning artifact in C92. Synthetic sense mRNA was transcribed *in vitro* from *Spe* I-linearized hH1 template as described (14).

Stage V or VI oocytes were microinjected with 30–50 ng of synthetic hH1 mRNA and studied after 3–10 days. Na^+ currents were measured either by two-microelectrode voltage clamp (14) or by patch clamp with outside-out patches (3). The bath solution contained 116 mM NaCl, 2 mM KCl, 1.8 mM $CaCl_2$, 2 mM $MgCl_2$, and 5 mM Hepes (pH 7.6). For

Abbreviations: NaCh, sodium channel; TTX, tetrodotoxin; TTX-I, TTX-insensitive; UT, untranslated; ID, interdomain; *I–V*, current–voltage; nt, nucleotide(s).

‖To whom reprint requests should be addressed at: 233 Anatomy Chemistry, 36th & Hamilton Walk, Philadelphia, PA 19104-6059.

**The sequence reported in this paper has been deposited in the GenBank data base (accession no. M77235).

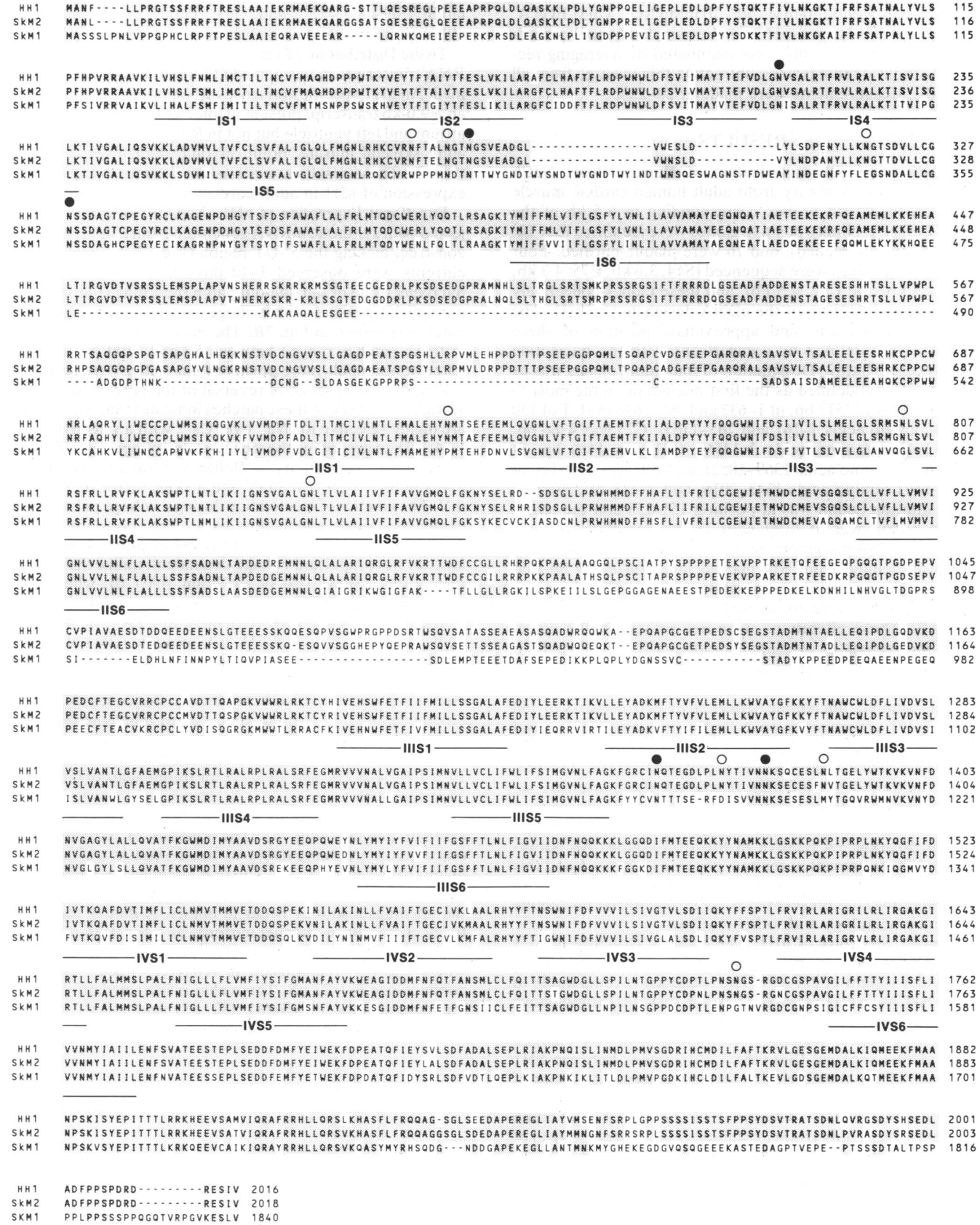

FIG. 1. Amino acid sequence of hH1, deduced from its cloned cDNA, is compared to sequences of rSkM1 (13) and rSkM2 (15). Identical amino acid residues are shaded. The suggested locations of the six transmembrane α-helices within each domain are designated by horizontal lines. Potential extracellular consensus glycosylation sites are indicated by circles (solid circles indicate sites conserved in all known NaChs).

patch clamp experiments, the vitelline membrane was removed by hyperosmotic stripping (17). The bathing solution contained 150 mM NaCl, 2 mM KCl, 1.5 mM $CaCl_2$, 1 mM $MgCl_2$, 10 mM glucose, and 10 mM Hepes (pH 7.4). The pipet

solution contained 130 mM CsF, 10 mM CsCl, 5 mM EGTA, and 10 mM Cs-Hepes (pH 7.3). For single-channel recordings, capacity transients were eliminated by averaging records without openings and subtracting this average from all records. Measurements were made at 20–22°C.

RESULTS

Isolation and Characterization of Human Heart NaCh cDNAs. A cDNA library from adult human cardiac muscle was screened with probes corresponding to 6.5 kb of the rSkM2 cDNA. Ninety positive clones were identified (6×10^5 recombinants screened), and 16 were plaque-purified. Four overlapping clones were sequenced (S14, 3.6 kb; C75, 4.3 kb; C21, 1.5 kb; and C92, 4.5 kb), and these clones collectively encompassed 8491 bp of the cDNA designated as hH1. The identity, orientation, and approximate position of these cDNAs were defined by comparisons with the nucleotide sequence of rSkM2. Designation of individual clones was as follows (nt 1 is defined as the first nucleotide in the most 5′ clone): S14 was 3517 bp, nt 1–632 and 762–3646 (5′-UT of 150 bp and amino acids 1–161 and 205–1165); C75 was 4366 bp, nt 152–4518 (amino acids 2–1456); C21 was 1450 bp, nt 4257–5707 (amino acids 1369–1852); and C92 was 4530 bp, nt 3980–8491 (amino acids 1343–2016, and 3′-UT of 2293 bp). The initiation codon was at position 151–153 and the termination codon was at 6199–6201 in the complete hH1 sequence. A 129-bp segment (nt 633–761; amino acids 162–204) that was deleted from S14 and an insertion of 19 bp that introduced a premature termination codon in C92 (insertion follows nt 4962) were discovered and appeared to be cloning artifacts. These alterations were not present in the corresponding regions of overlapping clones C75 and C21. Full-length constructs containing one or both of these defects were nonfunctional in oocyte expression studies.

The complete nucleotide sequence of hH1 consists of 150 bp of 5′-UT sequence, an open reading frame of 6048 bp, and a 3′-UT region of 2293 bp that contains neither a polyadenylylation signal sequence nor a poly(dA) region. The predicted initiation site of hH1 resembles the consensus sequence for eukaryotic initiation sites only in the presence of a purine nucleotide (adenosine) at position −3 and a guanosine at position +4 relative to the start codon. An out-of-frame ATG is present at relative positions −8 to −6 and this is a constituent feature of all previously cloned NaChs. An extensive 3′-UT is present but bears no significant nucleotide sequence homology with other NaChs.

Primary Structure of hH1. The primary structure of hH1 (Fig. 1) consists of 2016 amino acids with a calculated molecular weight of 227,159. The sequence is comparable to other NaChs, with four large (226–288 residues) homologous domains, each containing at least six potential membrane spanning α-helical segments including a positively charged amphipathic segment (S4) (18). Comparisons between hH1 and each of the cloned NaChs reveal a consistent pattern of primary structure homology within the repeat domains and the interdomain (ID) 3–4 region. ID 1–2 and ID 2–3 are much less conserved; only rSkM2 exhibits a high degree (>80%) of amino acid sequence identity with these regions of hH1. In addition, the ID 1–2 region is 296 residues long, more similar to brain NaCh isoforms than the adult skeletal muscle isoform (rSkM1) or eel electroplax NaCh.

There are 14 potential sites for N-linked glycosylation in regions of hH1 predicted to be extracellular, all of which are conserved from rSkM2; 5 sites (residues 214, 291, 328, 1365, and 1380) are found in all cloned NaChs. Most of these sites are located within the S5–S6 interhelical regions of D1 and D3. Within predicted cytoplasmic domains, there are six consensus sites for cyclic nucleotide-dependent phosphorylation (Ser-483, -571, and -593; Thr-17, -977, and -1026) although none are universally present in other NaChs.

Tissue Distribution of hH1. The steady-state levels of hH1 RNA transcripts in various adult human tissues were examined. An hH1-specific antisense cRNA probe hybridizes with an ≈9.0-kb transcript present in total RNA isolated from right atrium and left ventricle but not in RNA isolated from human adult skeletal muscle, brain, myometrium, liver, or spleen (Fig. 2). These results are consistent with the tissue-specific expression of hH1 in adult cardiac muscle.

Functional Expression of hH1. *Xenopus* oocytes were injected with synthetic mRNA generated from a full-length hH1 construct lacking the 5′-UT region (Figs. 3–5). Typical Na^+ currents were observed 3–10 days later with either two-microelectrode or outside-out patch recording (Fig. 3*A*). The normalized peak current–voltage (*I–V*) relationship for six patches is shown in Fig. 3*B*. The maximum inward currents in these patches ranged between 89 and 1100 pA and activated at potentials more positive than −60 mV (maximum at −10 mV). The absence of reversal of the current at voltages as high as +90 mV in these patches indicates that the channels are highly selective for Na^+ over Cs^+, with a selectivity ratio >34:1. Data describing the steady-state voltage dependence of inactivation were fit by a Boltzmann distribution with a midpoint of −61.9 ± 0.3 mV and a slope factor of 7.7 ± 0.3 mV. The kinetics of inactivation during a voltage pulse usually exhibited a single exponential with a time constant (τ_h) that decreased ≈*e*-fold/53 mV with depolarization. Inactivation kinetics were rapid and voltage-dependent, unlike the currents from either rSkM1 (19) or rat brain IIA (20), which show abnormally slow inactivation in *Xenopus* oocytes.

The hH1 currents were insensitive to TTX (Fig. 4*A*), with an IC_{50} value of 5.7 ± 0.8 μM. μ-Conotoxin (100 nM), which blocks TTX-sensitive NaChs from skeletal muscle (5, 19), does not block the Na^+ current of hH1 when expressed in oocytes. Lidocaine (10 μM) produces a frequency-dependent block (Fig. 4*B*). In five oocytes, 10 μM lidocaine blocked 2 ± 2%, 21 ± 3%, and 37 ± 3% of the peak current at 0.5, 5, and 10 Hz, respectively. At 100 μM lidocaine, the block was 29 ± 7%, 54 ± 7%, and 70 ± 7% for frequencies of 0.5, 5, and 10 Hz (n = 3).

Single-channel currents were obtained for hH1 from outside-out patches (Fig. 5). The kinetics of activation and inactivation are comparable to those seen in patches from mammalian heart (21, 22). The first latencies to openings and the probability of late openings decrease with depolarization; the openings also may occur in bursts. A plot of the amplitudes of the single-channel currents as a function of voltage shows inward rectification. Between −20 and +10 mV, where the *I–V* relationship is relatively linear, the slope conductance is ≈22 pS. This value is intermediate between the conductance of rSkM1 (32 pS) and rSkM2 (10 pS) measured under identical conditions (Fig. 5).

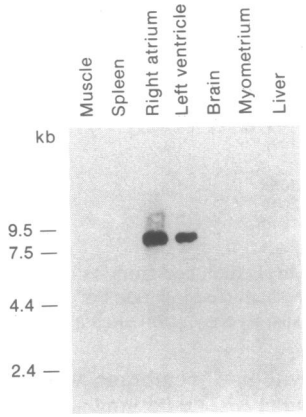

FIG. 2. Northern blot analysis of the tissue distribution of hH1 transcripts. Locations of RNA size standards (in kb) electrophoresed on the same gel are indicated to the left. The size of the hH1 transcript in atrium and ventricle is ≈9.0 kb.

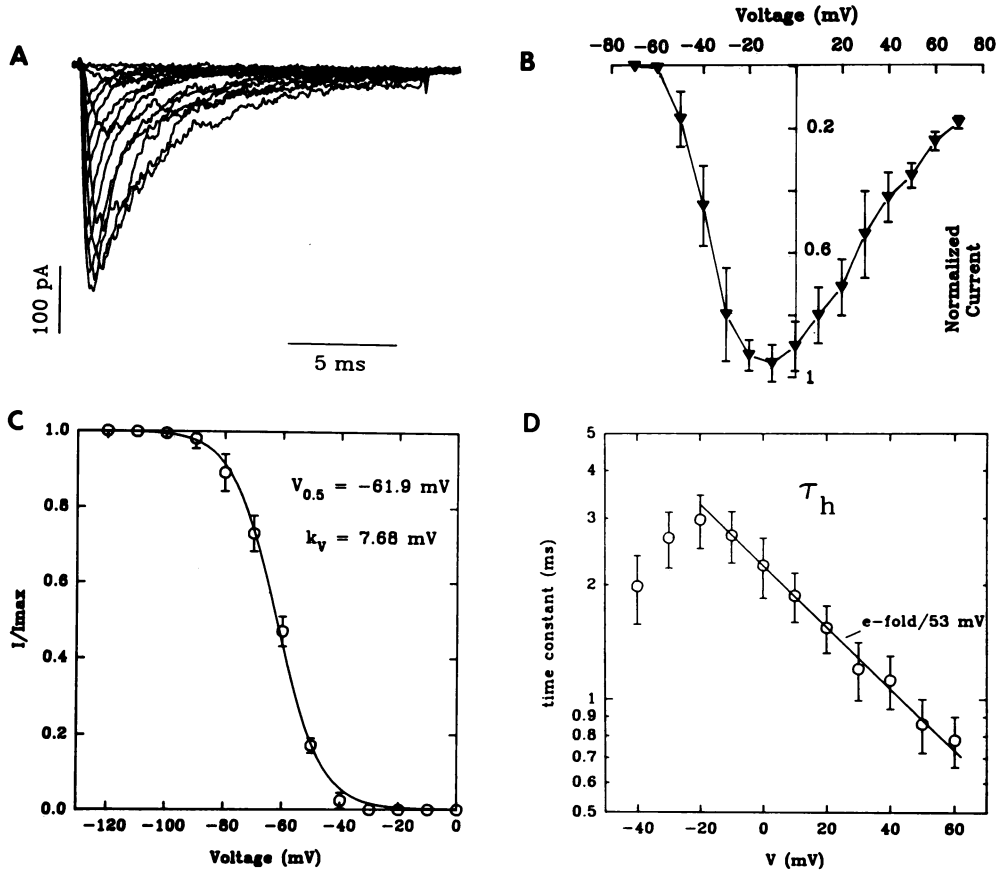

FIG. 3. Activation and inactivation of Na^+ currents of hH1 expressed in oocytes. (*A*) A family of Na^+ currents in a large outside-out patch. The holding potential was −120 mV, and capacity transients were removed by a P/8 procedure from the same holding potential. The currents were elicited by 26-ms pulses from −70 to +70 mV in 10-mV increments. (*B*) The normalized peak *I–V* relationship (mean ± SD) for six patches. (*C*) The steady-state inactivation curve for the data (mean ± SD) obtained with large outside-out patches from seven oocytes. The test potential was −30 mV, and the 45-ms prepulses ranged from −120 to 0 mV. The theoretical curve is a nonlinear least squares fit of the data by the formula $I/I_{max} = 1/\{1+\exp[(V-V_{0.5})/k_v]\}$, where I_{max} is the current measured from −120 mV. (*D*) Voltage dependence of τ_h, measured by fitting the decay of the current after the peak with a single exponential. Data (mean ± SEM) were analyzed from six patches.

DISCUSSION

At least six distinct isoforms of the voltage-dependent NaCh α subunit exist in rat brain, skeletal muscle, and heart. Based upon previously published observations (23, 24), it appears likely that a similar array of NaCh subtypes exists in the human genome. We characterize here a member of the human NaCh α-subunit multigene family, hH1.

The most striking aspect of the hH1 channel primary structure is its high level of similarity with rSkM2 (15) and the rat cardiac NaCh RH1 that appears to be identical to rSkM2 (25). The degree of primary structure identity that exists between human hH1 and rSkM2 (93.8%) is significantly greater than that between the two rat isoforms rSkM1 and rSkM2 (59%), which are coexpressed in skeletal muscle. These comparisons are particularly striking in the ID 1–2 and ID 2–3 regions where amino acid sequence identity between rSkM1 and rSkM2 is much lower (14 and 23%) than that between human hH1 and rSkM2 (88% for ID 1–2 and 84% for ID 2–3). This observation suggests that structural differences between NaCh isoforms have been conserved during evolution and are likely to be important physiologically.

The S5–S6 interhelical region in D1 has been postulated to contribute to the binding site for TTX. A comparison of the primary structure of this segment in TTX-I and TTX-sensitive NaChs is particularly interesting since a marked decrease in the affinity for TTX has been reported in rat brain II NaChs subjected to site-specific mutation at position 387 (Glu → Gln) in this region (26). Although the neutralization of negative charge produced by this mutation might interfere with binding of the cationic neurotoxins TTX and saxitoxin, a glutamate corresponding to Glu-387 is conserved in all known NaCh sequences including hH1 (Glu-375) and, therefore, cannot be a determinant of toxin binding. However, the adjacent asparagine residue that is present in all TTX-sensitive NaCh isoforms is replaced by arginine in both hH1(Arg-376) and rSkM2. This charge difference could contribute to the decreased affinity for TTX exhibited by these channels. Four additional residues in this region are conserved in the TTX-I isoforms but differ in charge from the consensus of the TTX-sensitive NaCh sequences; these include two additional positive residues (Lys-317 and Arg-340) and two negative residues (Glu-346 and Asp-349).

In spite of the structural and electrophysiological similarities between hH1 and rSkM2, there are two distinct functional differences. (*i*) hH1 is less sensitive to TTX block, with an apparent affinity (IC_{50} = 5.7 μM) almost 3 times lower than that found for rSkM2 (14). (*ii*) The amplitudes of the single-channel currents of hH1 are different than those found in rSkM2. The hH1 single-channel *I–V* curve shows inward rectification with a conductance near 0 mV of ≈22 pS (Fig. 5), whereas equivalent measurements in rSkM2 (Fig. 5; ref. 27) and in developing rat skeletal muscle (3) yield a linear *I–V* relation with a slope ≈10 pS. The simplest hypothesis for the difference between the two types of TTX-I channels is that the hH1 channel has more negative charge near the extracellular mouth of the pore than rSkM2. This charge could increase the local concentration of Na^+ (thus increasing the conductance) and of Ca^{2+}, known to block open Na^+ channels in a voltage-dependent manner (28). Calcium ions can produce the curvature in the *I–V* trace at negative potentials, where the block is enhanced due to the higher probability of Ca^{2+} residing in a blocking site in the pore. Four negatively charged residues in hH1 that replace neutral amino acids at corresponding positions of rSkM2 and that may lie at the extracellular mouth of the channel are located in the S5–S6 interhelical regions of domains 1 (Glu-302 and Glu-312), 2 (Asp-870), and 4 (Asp-1741).

The inactivation kinetics of expressed hH1 currents are rapid and closely resemble sodium currents observed in intact cardiac tissue. In contrast, functional expression of other cloned NaChs (rSkM1 and rat brain IIA) in *Xenopus* oocytes results in abnormally slow inactivation (19, 20). The

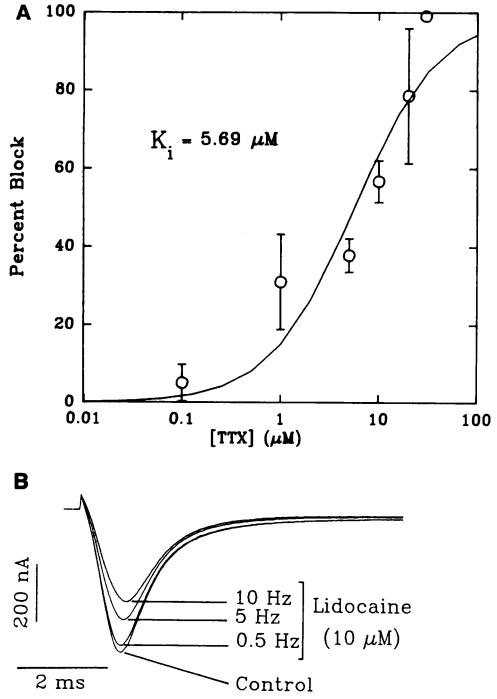

FIG. 4. Effect of NaCh blockers on hH1 currents in voltage-clamped oocytes. (*A*) Dose–response curve (mean ± SD) for TTX inhibition (at −30 mV) of hH1 current in seven oocytes. The theoretical curve is the best fit to a model for a one-site block with an IC_{50} of 5.7 μM. All toxin effects were completely reversible in these experiments. (*B*) Inhibition of hH1 currents by 10 μM lidocaine. Lidocaine block was examined using 16-ms pulses to −20 mV from a holding potential of −100 mV. The currents were measured as the peak amplitude on the 20th pulse at stimulus frequencies of 0.5, 5, and 10 Hz.

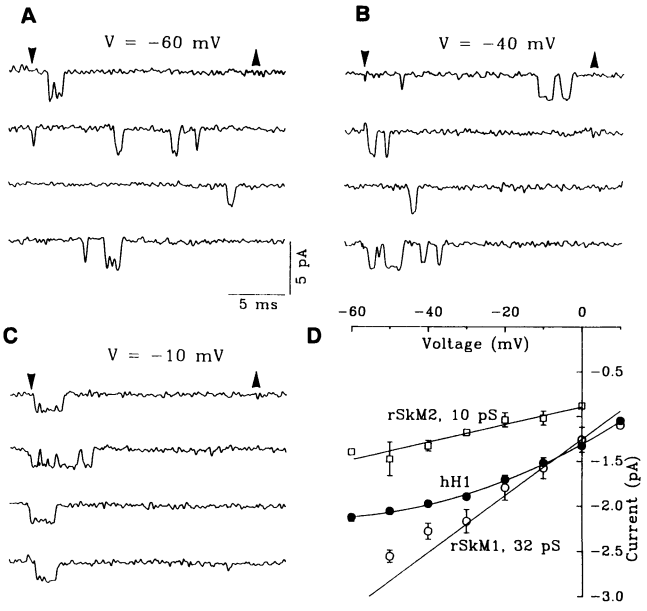

FIG. 5. Single-channel currents. Data traces obtained from an outside-out patch of an hH1-injected oocyte. Selected traces show openings elicited at −60 (*A*), −40 (*B*), and −10 (*C*) mV. The beginning and end of the pulses are indicated by the downward and upward arrows. (*D*) Amplitudes (mean ± SD) of the single-channel currents for this patch. Similar amplitudes were obtained in two other patches from two oocytes. This graph also shows the single-channel *I–V* relationships from oocytes injected with mRNA for rSkM1 (n = 4 patches, mean ± SEM) and rSkM2 (n = nine patches). Straight lines with indicated slopes are superimposed on the data for the rat NaChs.

fact that rSkM1 and rat brain IIA NaChs exhibit rapid inactivation kinetics when expressed in mammalian somatic cell lines (29, 30) suggests that abnormal behavior of expressed NaChs may occur because of differences in post-translational processing or lack of a modulating factor(s) in oocytes rather than differences in primary structure.

We are grateful for the technical contributions of Dr. Paul Brehm, Qiu Huang, and Berndt Fackler. This work was supported by grants from the National Institutes of Health (NS-18013), the Muscular Dystrophy Association (to R.L.B. and R.G.K.), the Research Foundation of the University of Pennsylvania, the Pew Foundation, and the Veterans Administration (to A.L.G.). M.E.G. was a Dana Neuroscience Fellow.

1. Trimmer, J. S. & Agnew, W. S. (1989) *Annu. Rev. Physiol.* **51**, 401–418.
2. Pappone, P. A. (1980) *J. Physiol. (London)* **306**, 377–410.
3. Weiss, R. E. & Horn, R. (1986) *Science* **233**, 361–364.
4. Harris, J. B. & Thesleff, S. (1971) *Acta Physiol. Scand.* **83**, 382–388.
5. Cruz, L. J., Gray, W. R., Olivera, B. M., Zeikus, R. D., Kerr, L., Yoshikami, D. & Moczydlowski, E. (1985) *J. Biol. Chem.* **260**, 9280–9288.
6. Haimovich, B., Schotland, D. L., Fieles, W. E. & Barchi, R. L. (1987) *J. Neurosci.* **7**, 2957–2966.
7. Rogart, R. B. (1986) *Ann. N.Y. Acad. Sci.* **479**, 402–430.
8. Brown, A. M., Lee, K. S. & Powell, T. (1981) *J. Physiol. (London)* **318**, 455–477.
9. Cohen, C. J., Bean, B. P., Colatsky, T. J. & Tsien, R. W. (1981) *J. Gen. Physiol.* **78**, 383–411.
10. Bean, B. P., Cohen, C. J. & Tsien, R. W. (1983) *J. Gen. Physiol.* **81**, 613–642.
11. Sutton, F., Davidson, N. & Lester, H. A. (1988) *Mol. Brain Res.* **3**, 187–192.
12. Tomaselli, G. F., Feldman, A. M., Yellen, G. & Marban, E. (1990) *Am. J. Physiol.* **258**, H903–H906.
13. Krafte, D., Volberg, W. A., Dillon, K. & Ezrin, A. M. (1991) *Proc. Natl. Acad. Sci. USA* **88**, 4071–4074.
14. White, M. M., Chen, L., Kleinfield, R., Kallen, R. G. & Barchi, R. L. (1991) *Mol. Pharmacol.* **39**, 604–608.
15. Kallen, R. G., Sheng, Z., Yang, J., Chen, L., Rogart, R. B. & Barchi, R. L. (1990) *Neuron* **4**, 233–242.
16. Chirgwin, J. M., Przybyla, A. E., MacDonald, R. J. & Rutter, W. J. (1979) *Biochemistry* **18**, 5294–5299.
17. Methfessel, C., Witzemann, V., Takahashi, T., Mishina, M., Numa, S. & Sakmann, B. (1986) *Pflügers Arch.* **407**, 577–588.
18. Guy, H. R. & Conti, F. (1990) *Trends Neurosci.* **13**, 201–206.
19. Trimmer, J. S., Cooperman, S. S., Tomiko, S. A., Zhou, J., Crean, S. M., Boyle, M. B., Kallen, R. G., Sheng, Z., Barchi, R. L., Sigworth, F. J., Goodman, R. H., Agnew, W. S. & Mandel, G. (1989) *Neuron* **3**, 33–49.
20. Auld, V. J., Goldin, A. L., Krafte, D. S., Marshall, J., Dunn, J. M., Catterall, W. A., Lester, H. A., Davidson, N. & Dunn, R. J. (1988) *Neuron* **1**, 449–461.
21. Kunze, D. L., Lacerda, A. E., Wilson, D. L. & Brown, A. M. (1985) *J. Gen. Physiol.* **86**, 691–719.
22. Cachelin, A. B., De Peyer, J. E., Kokubun, S. & Reuter, H. (1983) *J. Physiol. (London)* **340**, 389–401.
23. George, A. L., Ledbetter, D. H., Kallen, R. G. & Barchi, R. L. (1991) *Genomics* **9**, 555–556.
24. Litt, M., Luty, J., Kwak, M., Allen, L., Magenis, R. E. & Mandel, G. (1989) *Genomics* **5**, 204–208.
25. Rogart, R. B., Cribbs, L. L., Muglia, L. K., Kephart, D. D. & Kaiser, M. W. (1989) *Proc. Natl. Acad. Sci. USA* **86**, 8170–8174.
26. Noda, M., Suzuki, H., Numa, S. & Stühmer, W. (1989) *FEBS Lett.* **259**, 213–216.
27. Kallen, R. G., Chen, L., Gellens, M. E., George, A. L., Chahine, M., Horn, R. & Barchi, R. L. (1991) *Soc. Neurosci. Abstr.* **17**, 952.
28. Yamamoto, D., Yeh, J. Z. & Narahashi, T. (1984) *Biophys. J.* **45**, 337–344.
29. Ukomadu, C., Zhou, J., Sigworth, F. J. & Agnew, W. S. (1991) *Biophys. J.* **59**, 69a (abstr.).
30. Scheuer, T., Auld, V. J., Boyd, S., Offord, J., Dunn, R. & Catterall, W. A. (1990) *Science* **247**, 854–858.